

# Radiation Shielding Properties of recycled waste glass color doped powder cement pastes

Nuray Kutu\*

\* Süleyman Demirel University, Isparta-Turkiye

\* Corresponding Author Email: nuraykutu@gmail.com - ORCID: 0000-0002-8095-0051

## Article History:

DOI: 10.22399/ijasrar.55

Received: Nov. 12, 2025

Revised: Jan. 05, 2025

Accepted: Jan. 10, 2026

## Keywords:

Gamma-ray shielding,  
Glass,  
Cement,

**Abstract:** In the present study, the gamma-ray shielding performance of cement (CEM), green, brown, and transparent glass materials was systematically investigated over the photon energy range of 0.015–15 MeV. Key radiation attenuation parameters including mean free path (MFP), half-value layer (HVL), tenth-value layer (TVL), effective atomic number (Zeff), and radiation protection efficiency (R) were evaluated using the Phy-X/PSD computational platform. The obtained results demonstrate a strong dependence of shielding parameters on photon energy, governed by dominant interaction mechanisms such as photoelectric absorption, Compton scattering, and pair production. Cement exhibited the lowest MFP, HVL, and TVL values across the studied energy range, indicating superior shielding efficiency, while colored glass samples showed competitive attenuation performance, particularly at intermediate photon energies. These findings suggest that cement and glass-based materials can serve as effective and practical alternatives for gamma-ray shielding applications.

## 1. Introduction

Gamma photons have high penetration capability and therefore require engineered shielding solutions in laboratories, hospitals, industrial facilities, and nuclear installations [20–23]. Traditional shields (e.g., lead-based systems and heavy concretes) provide effective attenuation but raise concerns related to toxicity, weight, handling, and life-cycle sustainability, which has intensified research on alternative and recycled-material-based shields [10,18,23]. Cementitious matrices and recycled glass are attractive candidates because they can be manufactured at scale, incorporate waste streams, and show durable performance in built environments [12,15,17].

Photon attenuation in matter is governed by photoelectric absorption at low energies, Compton scattering at intermediate energies, and pair production at high energies; consequently, shielding metrics are strongly energy dependent [1,3,4]. Practical design indicators such as HVL and TVL, together with interaction descriptors such as Zeff, are widely reported to benchmark shielding materials and interpret the governing interaction mechanism [8,9,11,19]. Computational tools such as XCOM/WinXCom and Phy-X/PSD are extensively used to estimate these parameters from composition and density in a reproducible manner [2–6].

The present work provides a comparative assessment of cement and recycled waste glass with different colors (green, brown, and transparent) using MFP, HVL, TVL, Zeff, and R across 0.015–15 MeV. Beyond reporting curves, we quantitatively interpret thickness requirements at representative energies and connect trends to interaction physics and the relevant literature, in a style consistent with Radiation Physics and Chemistry reporting conventions [2,8,10,12,17].

## 2. Materials and Methods

The investigated materials comprise cement (CEM) and three glass types (green, brown, and transparent). The material chemical variability and densities used in the calculations are summarized in Table 1. All radiation shielding parameters were calculated using the Phy-X/PSD software. The linear attenuation coefficient ( $\mu$ ) was used to derive MFP, HVL, and TVL according to the following relations [1,5,23],

**Table 1.** Chemical variability and densities of cement and glass samples used in the Phy-X/PSD calculations

chemical variability	Cement (CEM) Wt %	Green Glass Wt %	Brown Glass Wt %	Transparent Glass Wt %
CaO	63,6	0	0	0
SiO <sub>2</sub>	19,5	69,2	68,3	68,8
Al <sub>2</sub> O <sub>3</sub>	4,4	2,5	3,8	2,6
Fe <sub>2</sub> O <sub>3</sub>	3,7	0,5	0,6	0,4
SO <sub>3</sub>	2,7	0,4	0,5	0,6
MgO	1,4	1,4	1,7	0,6
K <sub>2</sub> O	0,58	0	0	0
Na <sub>2</sub> O	0,56	13,2	13	13,1
ZnO	0	1,8	2,3	2
<b>Density (g/cm<sup>3</sup>)</b>	3.10	2.50	2.52	2.51

$$MFP = \frac{\mu}{1}$$

$$HVL = \frac{\ln(2)}{\mu}$$

$$TVL = \frac{\ln(10)}{\mu}$$

The effective atomic number (Zeff) was computed based on photon interaction cross-sections, considering photoelectric absorption, Compton scattering, and pair production processes [7,11,19]. Radiation protection efficiency (R) was calculated as:

$$R (\%) = (1 - \frac{I}{I_0}) \times 100$$

where I<sub>0</sub> and I denote the incident and transmitted photon intensities, respectively [16–18].

### 3. Results and Discussions

#### MFP (Mean Free Path)

As shown in Figure 1, MFP increases with photon energy for all materials, reflecting the decrease in interaction probability as energy rises, particularly from the photoelectric-dominated region to the Compton regime [1,3]. Cement consistently exhibits the smallest MFP values across the full energy range, which is primarily attributable to its higher density (Table 1) and correspondingly higher linear attenuation coefficient  $\mu$  (see LAC outputs) [10,23,25].

Numerically, the cement MFP increases from 1.883e-04 cm at 0.015 MeV to 0.1379 cm at 15 MeV, illustrating the expected reduction in attenuation with increasing energy. At 1.0 MeV, cement (MFP  $\approx$  0.0526 cm) remains lower than the brown glass (MFP  $\approx$  0.0651 cm), indicating reduced required mean interaction spacing and therefore improved shielding compactness [8,10,18].

#### HVL (Half-Value Layer)

HVL trends in Figure 2, mirror the MFP behavior because both parameters scale inversely with  $\mu$ . HVL provides a thickness-based metric directly relevant to design and is routinely used in medical and industrial shielding evaluations [23]. Across energies, cement yields the lowest HVL, implying that smaller thickness is required to reduce the incident photon intensity by 50% compared with the recycled

glass samples. At 0.015 MeV, cement HVL is  $1.305\text{e-}04$  cm, while brown and transparent glasses are  $3.573\text{e-}04$  and  $3.298\text{e-}04$  cm, respectively (Figure 2). At 1.0 MeV, cement HVL increases to  $\approx 0.0365$  cm, which remains  $\sim 19.2204\%$  lower than brown glass ( $\approx 0.0451$  cm). Such relative separations are consistent with reports that higher-density cementitious shields provide reduced HVL values compared with conventional building materials, especially in the low-to-intermediate energy region [10,12,18,25].

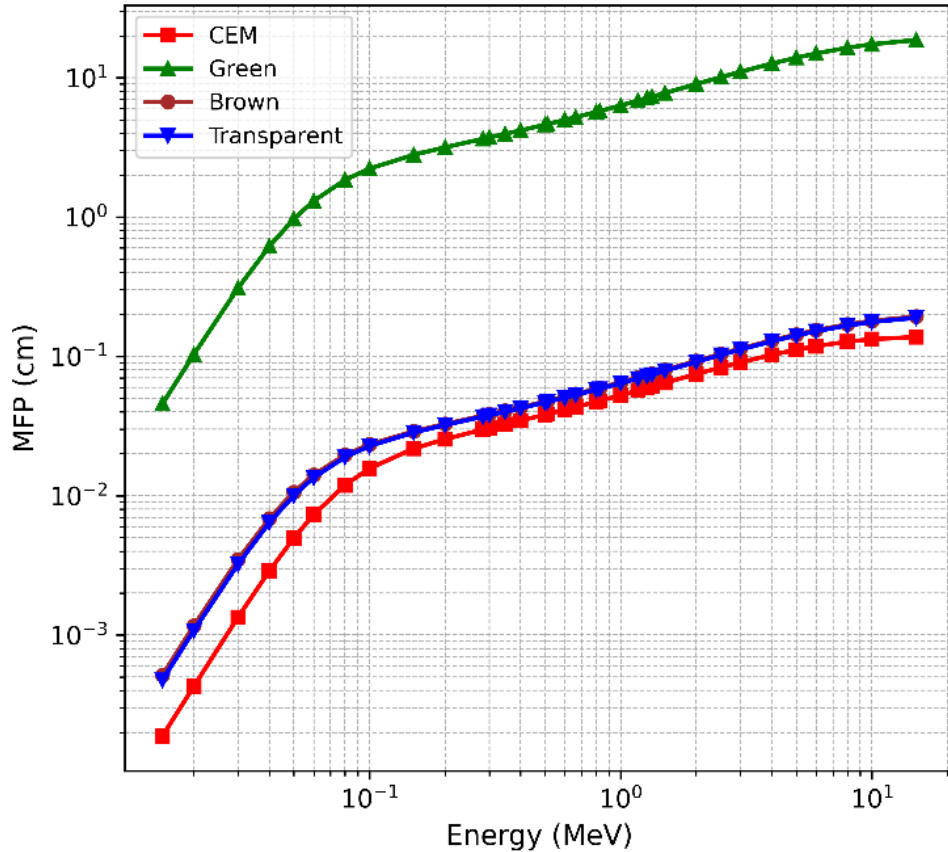
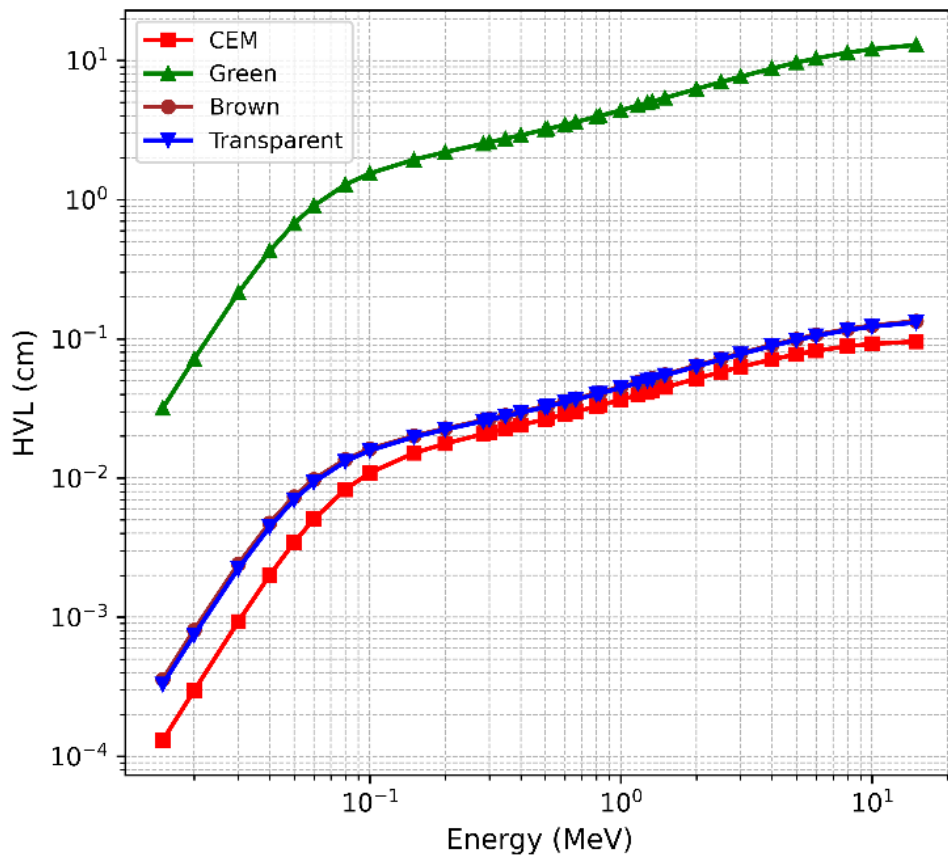


Figure 1. Log–log variation of mean free path (MFP) versus photon energy for cement and glass samples.

## TVL (Tenth-Value Layer)

TVL is particularly important for engineering design because it corresponds to one order-of-magnitude attenuation ( $I/I_0 = 0.1$ ) [23]. Figure 3, shows that TVL increases with energy for all materials, with a relatively slower increase at higher energies as interaction mechanisms evolve [1,4]. Cement exhibits systematically lower TVL values than all glass samples, indicating more efficient shielding per unit thickness. Quantitatively, at 0.015 MeV cement TVL is  $4.335\text{e-}04$  cm, whereas brown and transparent glasses are 0.0012 and 0.0011 cm, respectively. At 1.0 MeV cement TVL is  $\approx 0.1211$  cm compared to  $\approx 0.1499$  cm (brown) and  $\approx 0.1477$  cm (transparent), corresponding to reductions of  $\sim 19.2204\%$  and  $\sim 18.0208\%$ , respectively. These reductions are consistent with the established role of density and composition in lowering the required shielding thickness for cement-based systems [10,23,25]. The green glass sample shows substantially higher TVL values across the full range (Figure 3), implying much larger thickness requirements for equivalent attenuation. While glass systems can achieve competitive performance when heavy oxides are incorporated, many common waste-glass compositions remain less effective than dense cementitious shields unless modified by high-Z additives, as reported for various glass families [8,9,13–17]. To support direct engineering interpretation, Table 2 lists TVL values at representative energies frequently used in shielding assessments (e.g., 0.662 MeV for  $^{137}\text{Cs}$ , 1.25 MeV for  $^{60}\text{Co}$  average line) [23]. At 0.662 MeV, cement TVL is  $\approx 0.0996$  cm, which is  $\sim 19.3544\%$  lower than brown glass ( $\approx 0.1235$  cm) and  $\sim 18.1489\%$  lower than transparent glass ( $\approx 0.1216$  cm).



**Figure 2.** Log–log variation of half-value layer (HVL) versus photon energy for cement and glass samples

At 1.25 MeV, cement TVL remains lower ( $\approx 0.1355$  cm) than both brown ( $\approx 0.1677$  cm) and transparent glass ( $\approx 0.1652$  cm), supporting the conclusion that cement provides more compact shielding thickness requirements in typical gamma-source energy ranges [10,23,25].

### Zeff (Effective Atomic Number)

Figure 4, shows that Zeff decreases from low energies to intermediate energies and then tends to stabilize, consistent with the transition from photoelectric absorption to Compton scattering dominance and subsequently increasing contribution from pair production at high energies [1,3,4,19]. Cement exhibits higher Zeff than the glass samples at low energies (e.g.,  $\sim 18.69$  at 0.015 MeV), which supports its superior attenuation where the photoelectric effect is strongly dependent on atomic number [1,11]. At 0.015 MeV, Zeff is 18.6885 (cement) versus 15.4786–14.7467 for the glass samples (Figure 1d). At 1.0 MeV, Zeff values converge (cement  $\approx 12.5686$ ), reflecting reduced Z-sensitivity in the Compton region [1,3]. Similar Zeff evolution with energy has been reported for a variety of composite and glass shielding materials, providing confidence in the consistency of the present calculations [7,8,11,13,19].

**Table 2.** Interpolated TVL values (cm) at representative photon energies for the investigated materials.

Energy (MeV)	CEM	GREEN	BROWN	TRANSPARENT
0.662	0.0996	11.9921	0.1235	0.1216
1.000	0.1211	14.5629	0.1499	0.1477
1.250	0.1355	16.2886	0.1677	0.1652
2.000	0.1718	20.7301	0.2134	0.2103
5.000	0.2570	32.0515	0.3306	0.3252

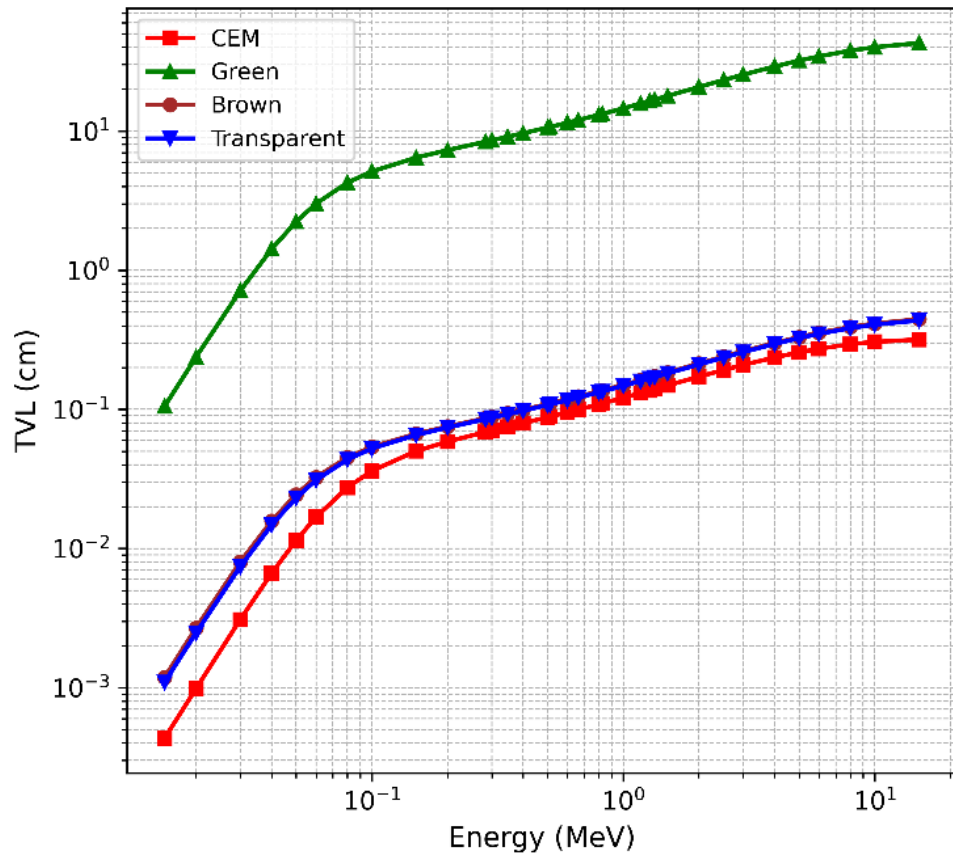


**Figure 3.** Log–log variation of tenth-value layer (TVL) versus photon energy for cement and glass samples.

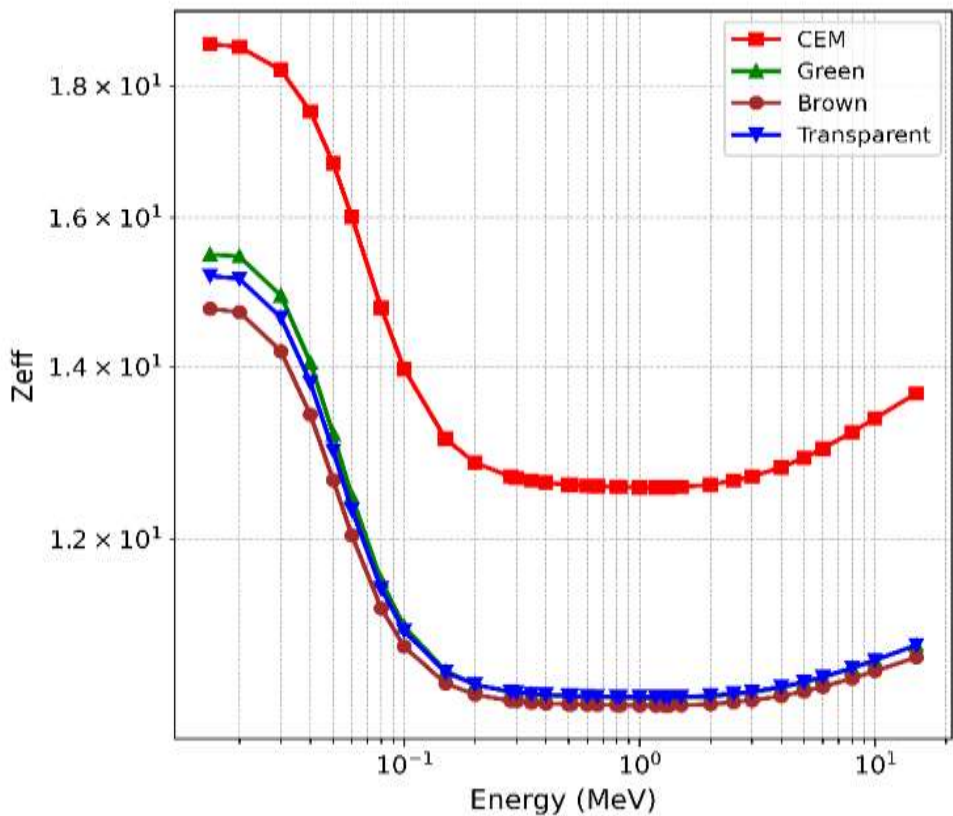


**Figure 4.** Semi-log variation of effective atomic number (Zeff) versus photon energy for cement and glass samples

## R (Radiation Protection Efficiency)

Radiation protection efficiency (R) captures the fraction of attenuated photons for a defined thickness and therefore decreases with increasing energy for all materials (Figure 5), consistent with a declining interaction probability at higher energies [16–18]. Cement maintains higher R values across most of the studied range, aligning with its lower MFP/HVL/TVL values. For example, at 0.05 MeV, R is 0.2506% for cement compared with 0.4495% (brown) and 0.4294% (transparent). At 1.0 MeV, cement yields R  $\approx$  0.9987% while brown and transparent glasses yield  $\approx$  0.9995% and  $\approx$  0.9994%. These trends agree with the broader shielding literature showing that R decreases with energy and increases with density/effective interaction probability for a fixed thickness [16–18,23].

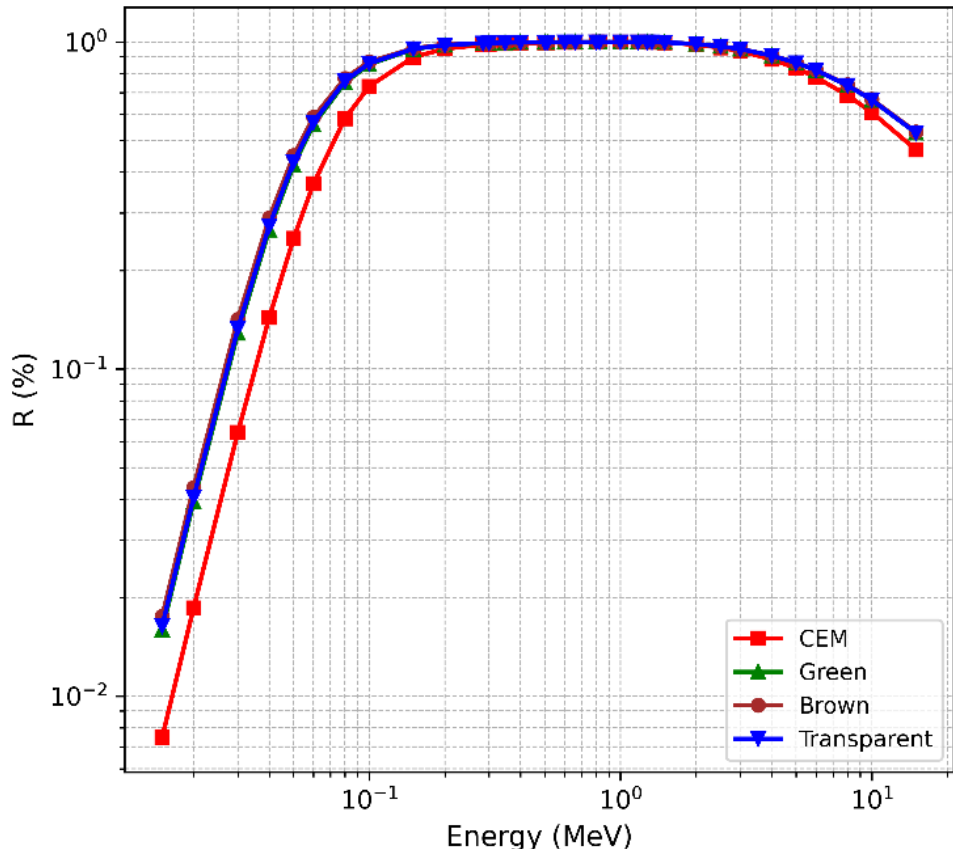


**Figure 5.** Log–log variation of radiation protection efficiency (R) versus photon energy for cement and glass samples.

## 4. Conclusions

Using Phy-X/PSD calculations over 0.015–15 MeV, cement demonstrated the most effective gamma-ray attenuation among the investigated materials, yielding the lowest MFP, HVL, and TVL values throughout the energy range [10,23,25]. Representative-energy analysis (Figure 2 and Table 2) further confirmed reduced thickness requirements for cement in common gamma-source energy windows (0.662–5 MeV) [23]. Among recycled glasses, brown and transparent samples show broadly comparable shielding behavior, while the green glass sample exhibits substantially higher thickness requirements in the present dataset. Overall, the multi-parameter framework (MFP/HVL/TVL/Zeff/R) provides a reproducible basis for comparing cement and waste-glass candidates, and supports sustainable design considerations when combined with mechanical and environmental requirements [12,15,17].

## . Author Statements:

- **Ethical approval:** The conducted research is not related to either human or animal use.
- **Conflict of interest:** The authors declare that they have no known competing financial interests or personal relationships that could have appeared to influence the work reported in this paper
- **Acknowledgement:** The authors acknowledge the use of the Phy-X/PSD platform for radiation shielding calculations.
- **Author contributions:** The authors declare that they have equal right on this paper.
- **Funding information:** The authors declare that there is no funding to be acknowledged.
- **Data availability statement:** The data that support the findings of this study are available on request from the corresponding author. The data are not publicly available due to privacy or ethical restrictions.

## References

- [1]. Hubbell, J. H., & Seltzer, S. M. (1995). *Tables of X-ray mass attenuation coefficients and mass energy-absorption coefficients*. National Institute of Standards and Technology.
- [2]. Şakar, E., Özpolat, Ö. F., Alim, B., Sayyed, M. I., & Karabulut, A. (2020). Phy-X/PSD: Development of a user-friendly online software for calculation of parameters relevant to radiation shielding and dosimetry. *Radiation Physics and Chemistry*, 166, 108496. <https://doi.org/10.1016/j.radphyschem.2019.108496>
- [3]. National Institute of Standards and Technology. (2026). *XCOM: Photon cross sections database*. <https://physics.nist.gov/xcom>
- [4]. Berger, M. J., & Hubbell, J. H. (1987). *XCOM: Photon cross sections on a personal computer* (NBSIR 87-3597). National Bureau of Standards.
- [5]. Gerward, L., Guilbert, N., Jensen, K. B., & Levring, H. (2004). WinXCom—A program for calculating X-ray attenuation coefficients. *Radiation Physics and Chemistry*, 71, 653–654. <https://doi.org/10.1016/j.radphyschem.2004.04.040>
- [6]. Gerward, L., Guilbert, N., Jensen, K. B., & Levring, H. (2001). X-ray absorption in matter: Reengineering XCOM. *Radiation Physics and Chemistry*, 60, 23–24. [https://doi.org/10.1016/S0969-806X\(00\)00350-1](https://doi.org/10.1016/S0969-806X(00)00350-1)
- [7]. Akkurt, I. (2009). Effective atomic numbers for Fe–Mn alloy using transmission experiment. *Chinese Physics B*, 18, 4217–4221. <https://doi.org/10.1088/1674-1056/18/10/046>
- [8]. Singh, V. P., & Badiger, N. M. (2012). Gamma-ray attenuation and shielding parameters of bismuth borate glasses. *Nuclear Instruments and Methods in Physics Research Section B*, 274, 68–73. <https://doi.org/10.1016/j.nimb.2011.12.015>
- [9]. El-Khayatt, A. M. (2011). Attenuation coefficients of glass systems containing heavy elements. *Annals of Nuclear Energy*, 38, 218–224. <https://doi.org/10.1016/j.anucene.2010.09.010>
- [10]. Bashter, I. I. (1997). Calculation of radiation attenuation coefficients for shielding concretes. *Annals of Nuclear Energy*, 24, 1389–1401. [https://doi.org/10.1016/S0306-4549\(97\)00003-0](https://doi.org/10.1016/S0306-4549(97)00003-0)
- [11]. Kurudirek, M. (2017). Effective atomic numbers and photon buildup factors in some shielding materials. *Radiation Physics and Chemistry*, 140, 136–144. <https://doi.org/10.1016/j.radphyschem.2017.02.018>
- [12]. Oto, B., Yilmaz, M., Kavaz, E., & Karaman, M. (2018). Gamma-ray attenuation properties of concrete and building materials. *Progress in Nuclear Energy*, 109, 94–102. <https://doi.org/10.1016/j.pnucene.2018.05.006>
- [13]. Rammah, Y. S., El-Agawany, F. I., & Sayyed, M. I. (2020). Evaluation of gamma-ray shielding parameters for phosphate glasses. *Ceramics International*, 46, 20835–20842. <https://doi.org/10.1016/j.ceramint.2020.05.190>
- [14]. Issa, S. A. M., Sayyed, M. I., Kurudirek, M., & Dong, M. G. (2018). Radiation shielding and optical properties of heavy metal oxide glasses. *Ceramics International*, 44, 18635–18641. <https://doi.org/10.1016/j.ceramint.2018.07.028>
- [15]. Al-Buriahi, M. S., Singh, V. P., Tonguc, B. T., & Sayyed, M. I. (2020). Radiation shielding performance of tellurite/borate glass systems. *Materials Chemistry and Physics*, 243, 122640. <https://doi.org/10.1016/j.matchemphys.2019.122640>
- [16]. Sayyed, M. I., Lakshminarayana, G., Kityk, I. V., Mahdi, M. A., & Dong, M. G. (2017). Shielding features of lead-free bismuth glass systems. *Journal of Alloys and Compounds*, 695, 3191–3199. <https://doi.org/10.1016/j.jallcom.2016.11.102>
- [17]. Al-Hadeethi, Y., & Sayyed, M. I. (2019). Effect of composition on gamma-ray shielding of glass materials. *Applied Radiation and Isotopes*, 150, 114–120. <https://doi.org/10.1016/j.apradiso.2019.04.040>
- [18]. Korkut, T. (2012). Photon interaction parameters and shielding performance of building materials. *Radiation Physics and Chemistry*, 81, 202–207. <https://doi.org/10.1016/j.radphyschem.2011.10.008>
- [19]. Manohara, S. R., & Hanagodimath, S. M. (2007). Studies on effective atomic numbers and attenuation in composite materials. *Nuclear Instruments and Methods in Physics Research Section B*, 258, 321–328. <https://doi.org/10.1016/j.nimb.2007.02.095>
- [20]. International Atomic Energy Agency. (2014). *Radiation protection and safety of radiation sources: International basic safety standards (GSR Part 3)*.

- [21]. International Commission on Radiological Protection. (2007). *The 2007 recommendations of the ICRP* (Publication 103).
- [22]. United Nations Scientific Committee on the Effects of Atomic Radiation. (2020). *Sources, effects and risks of ionizing radiation*. United Nations.
- [23]. National Council on Radiation Protection and Measurements. (2004). *Structural shielding design and evaluation for medical use of X rays and gamma rays* (NCRP Report No. 147).
- [24]. Akkurt, I., Basyigit, C., Kilincarslan, S., & Mavi, B. (2006). The shielding of gamma rays by concretes produced with barite. *Progress in Nuclear Energy*, 48, 397–404.  
<https://doi.org/10.1016/j.pnucene.2005.09.002>
- [25]. Mahmoud, K. A., & Sayyed, M. I. (2019). Gamma-ray shielding properties of cement-based materials. *Construction and Building Materials*, 215, 970–977. <https://doi.org/10.1016/j.conbuildmat.2019.04.177>
- [26]. Tekin, H. O. (2017). Monte Carlo evaluation of photon shielding parameters. *Radiation Physics and Chemistry*, 139, 1–7. <https://doi.org/10.1016/j.radphyschem.2017.01.020>
- [27]. Kaky, K. M., & Sayyed, M. I. (2021). Assessment of radiation shielding properties of glass systems. *Silicon*, 13, 985–993. <https://doi.org/10.1007/s12633-020-00457-5>
- [28]. Singh, K., Singh, H., Sharma, V., Nathuram, R., Khanna, A., Kumar, R., & Bhatti, S. S. (2002). Gamma-ray attenuation coefficients in bismuth borate glasses. *Nuclear Instruments and Methods in Physics Research Section B*, 194, 1–6. [https://doi.org/10.1016/S0168-583X\(02\)00720-0](https://doi.org/10.1016/S0168-583X(02)00720-0)
- [29]. El-Mallawany, R. (2013). *Tellurite glasses handbook: Physical properties and data*. CRC Press.  
<https://doi.org/10.1201/b16183>
- [30]. Rammah, Y. S., El-Agawany, F. I., & Sayyed, M. I. (2018). Radiation shielding characteristics of lead-free borate glasses. *Journal of Non-Crystalline Solids*, 503–504, 224–230.  
<https://doi.org/10.1016/j.jnoncrysol.2018.09.024>